CALIBRATION OF A SIMPLE, LOW COST, 3D LASER LIGHT-SECTIONING SCANNER SYSTEM FOR BIOMEDICAL PURPOSES

Beverly D. Bradley[1], Adrian D.C. Chan[1], John D. Hayes[2]
[1]*Systems and Computer Engineering, Carleton University*
[2]*Mechanical and Aerospace Engineering, Carleton University*

ABSTRACT

Three dimensional scanning is gaining popularity in the biomedical field for various applications where a 3D model of the external features of an anatomical part is beneficial. An analysis of two different calibration techniques, an analytical method and a least squares method, for a simple, low cost, 3D laser light-sectioning scanner system is presented. Both methods are evaluated according to their ability to cope with noise in the input calibration data. The least squares approach shows better performance under noisy data conditions; however both appear suitable for the given application. Directions for future work are also discussed.

INTRODUCTION

For many years, three dimensional (3D) scanning systems for acquiring the external shape features of arbitrary objects have been used in industry for applications such as reverse engineering and part inspection. More recently, 3D scanning has been used in the biomedical field for applications such as orthodontic treatment planning [1], cranial deformation research [2], cartilage morphology studies [3], and anthropometric data collection [4]. The potential exists to expand the biomedical uses of 3D models even further, by continuing to develop simpler, more cost effective systems for acquiring external shape features of biological objects.

A simple, low cost, 3D scanning system is being developed for biomedical purposes which employs the laser light-sectioning technique [5]. This technique involves measuring the position of an object's surface profile by capturing images of where the profile intersects a plane of laser light projected onto the object from different angles (Fig. 1). A single planar section of an object is obtained from multiple profiles captured about the z-axis. A 3D image of the object is formed by stacking multiple planar sections along the z-axis.

Since the camera used to capture images is located at a fixed angle α to the laser plane, an important part of this system is the calibration procedure required to eliminate the linear portion of the camera perspective distortion for points lying along the imaged laser trace (in the x-y plane).
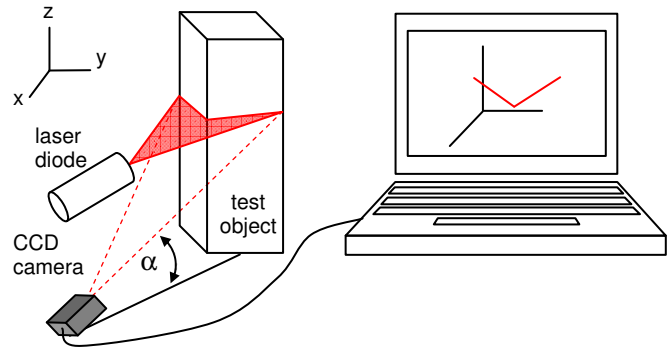
Figure 1: Laser light-sectioning system diagram

This paper presents an analysis of two different calibration techniques for finding a homogeneous transformation matrix, *T,* which can be used to remove this perspective distortion: 1) an analytical method using projective geometry; and 2) a least squares (LS) approach involving the Direct Linear Transformation (DLT) algorithm. Both are evaluated in terms of their performance under noisy data conditions. The study looks at how accurately the calculated transformation matrix maps points from the image of the calibration grid to their ideal location on the grid in a Cartesian coordinate system. Directions for future work are also discussed.

METHODS

All recorded laser traces lie in the laser plane (x-y plane). Hence, the images can be calibrated by superimposing a calibration grid of known dimensions on this laser plane and recording an image. Fig. 2 shows such a grid with $1mm^2$ grid squares; the highlighted quadrilateral demonstrates the camera distortion. A homogeneous transformation matrix, *T*, is computed by taking points from this image at certain grid locations and mapping them to their corresponding points on the known calibration grid in Cartesian space. The two methods investigated for calculating *T* are described below:
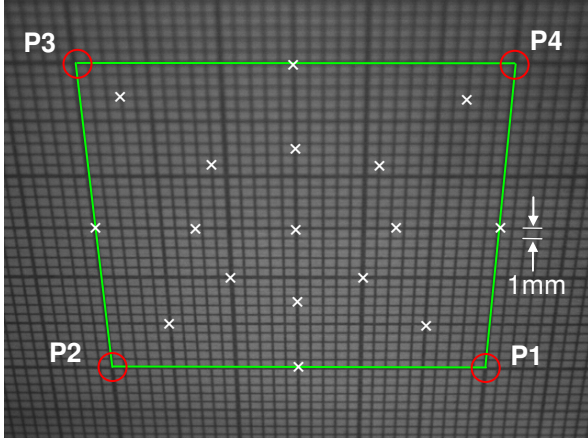
Figure 2: Calibration grid superimposed on laser plane. Highlighted quadrilateral shows perspective distortion due to the camera's incline of $\alpha = 40°$. Corner points P1 to P4 for calibration are indicated, as are an additional 16 points for the DLT LS method.

Analytical Method

The analytical method, described further in [5], can be represented compactly by the linear transformation presented in (1).

$$\rho W = Tw \tag{1}$$

where $W(X, Y, 1)$ are the coordinates of a point in the image plane, $w(u, v, 1)$ are the coordinates of the same point on the distorted calibration grid image, and ρ represents a scaling factor which, when factored out, leaves the point W which corresponds to a point in a Cartesian coordinate system. The coordinates of four known points, along with those of their corresponding images on the distorted calibration grid (P1–P4 in Fig. 2), are enough to uniquely identify the 8 independent elements of the homogeneous transformation matrix, T. All other image points can then be transformed from the projective into the Cartesian plane using T.

Direct Linear Transform Least Squares Method

For the DLT LS method, the same notation as given in (1) can be used; the matrix T is referred to as the DLT matrix. The method for finding T in this case is as follows: starting from (1), the expanded notation is shown in (2).

$$\begin{bmatrix} \rho X \\ \rho Y \\ \rho \end{bmatrix} = \begin{bmatrix} a_{11} & a_{12} & a_{13} \\ a_{21} & a_{22} & a_{23} \\ a_{31} & a_{32} & a_{33} \end{bmatrix} \begin{bmatrix} u \\ v \\ 1 \end{bmatrix} \tag{2}$$

Multiplying out the right hand side, and dividing the first and second equations by the last equation removes the homogeneous scale factor ρ as shown in (3):

$$\begin{bmatrix} X \\ Y \\ 1 \end{bmatrix} = \begin{bmatrix} \dfrac{a_{11}u + a_{12}v + a_{13}}{a_{31}u + a_{32}v + a_{33}} \\ \dfrac{a_{21}u + a_{22}v + a_{23}}{a_{31}u + a_{32}v + a_{33}} \\ 1 \end{bmatrix} \tag{3}$$

Rearranging (3) with respect to the DLT matrix parameters a_{ij}, $(i,j=1,2,3)$ and setting $a_{33} = 1$ gives (4) for any pair k of control points:

$$\begin{bmatrix} u_k & v_k & 1 & 0 & 0 & 0 & -X_k u_k & -X_k v_k \\ 0 & 0 & 0 & u_k & v_k & 1 & -Y_k u_k & -Y_k v_k \end{bmatrix} \begin{bmatrix} a_{11} \\ a_{12} \\ a_{13} \\ a_{21} \\ a_{22} \\ a_{23} \\ a_{31} \\ a_{32} \end{bmatrix} = \begin{bmatrix} X_k \\ Y_k \end{bmatrix} \tag{4}$$

Since each set of control point pairs gives two such equations, $2m$ equations are obtained from m calibration point pairs. These can be represented in standard matrix form as $A_{2m\times8}x_{8\times1}=b_{2m\times8}$, where x is the column vector of DLT matrix parameters and b is a column vector of known calibration coordinates. At least $m = 4$ control point pairs are necessary to solve for the 8 DLT parameters in the above system. However, if $m > 4$, the system is over-constrained and a least squares solution can be applied. The pseudo-inverse of A, $A^+ = (A^TA)^{-1}A^T$, is used to obtain the least squares solution $x = A^+b$. This approach is anticipated to be beneficial for coping with noise that may be associated with acquiring grid point locations from the image for the control point pairs.

Experimental Methods

This analysis examines how the two methods of finding T behave with varying amounts of noise associated with the points taken from the camera image of the calibration grid in order to compute T. This noise could arise from issues such as minor inaccuracies in the calibration grid or artifacts in the image processing methods used to isolate grid corner locations and identify their coordinates within the

image. A test scenario was generated using a transformation matrix known to be representative of the mapping required to transform points for the laser light-sectioning system presented in [5]. Using the inverse of *T* to transform the four corners of a known square on the calibration grid, the corresponding point pair locations, as they would appear on the distorted image of the grid, were generated (P1-P4 on Fig.2). This produced a complete set of ideal control point pairs and the transformation that maps between the two. In addition to these 4 point pairs, 16 other point pairs were generated for use with the DLT LS method (×'s on Fig. 2).

The noise associated with identifying grid intersections would be random in nature and is not expected to exceed the width of a grid line, which is approximately 3 pixel units in our system (at the centre of the calibration grid image). Assuming a Gaussian distribution, and setting 2 standard deviations to be 3 pixel units, the variance is $\sigma^2 = 2.25$. Random Gaussian noise with zero-mean and noise variances above and below 2.25 ($\sigma^2 = 0.140625, 0.28125, 0.5625, 1.125, 2.25, 4.5, 9,$ and 18) was added to the 4 corner points of the distorted quadrilateral and the extra 16 points for the DLT LS method, in both the x and y directions. Noisy points were then inputted into the 2 calibration algorithms. The DLT LS method was used twice; once with 4 control point pairs and once with 20 control point pairs. In total, 20 trials were performed at each of the 8 noise variance levels for each tested calibration algorithm. The radial difference between the transformed points and their known locations according to the ideal mapping was averaged across all 20 trials at each σ^2 value for the 4 corner grid points (P1-P4). This average radial error was then scaled according to the scaling used for the test object imaged in [5] in order to present the results in units of mm.

Using SPSS, a three-way analysis of variance (ANOVA) test was conducted on the results to determine whether or not calibration method, point location, and/or noise level have a significant effect on the radial error of transformed points. Pairwise comparisons between factors were performed using the Tukey and Dunnett's T3 post-hoc tests to determine which calibration methods, point locations, and/or noise levels produce mean radial errors significantly different from the others.

RESULTS

Figs. 3, 4 and 5 show error results at 8 different magnitudes of noise for the analytical method, the DLT LS method using 4 control point pairs, and the DLT LS method using 20 control point pairs, respectively. Errors for the 4 test corner points are shown as

separate data sets. Average error across the 20 trials is plotted and standard deviations for the 20 trials are indicated with bars.
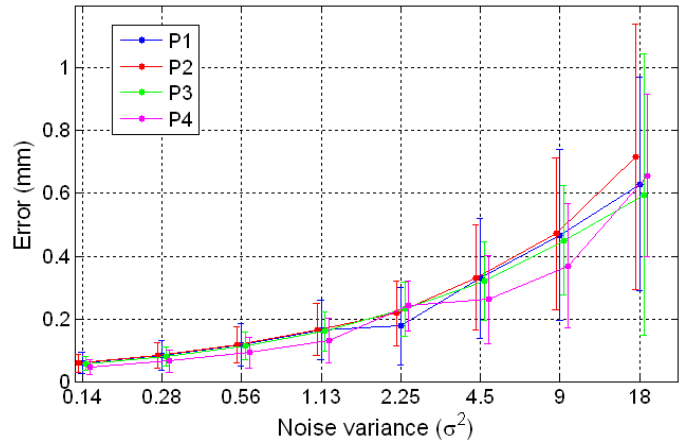
Figure 3: Error results for analytical method.
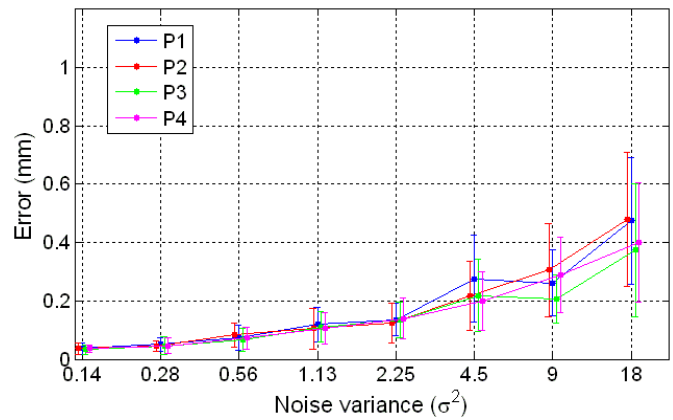
Figure 4: Error results for DLT least squares method using 4 control point pairs.
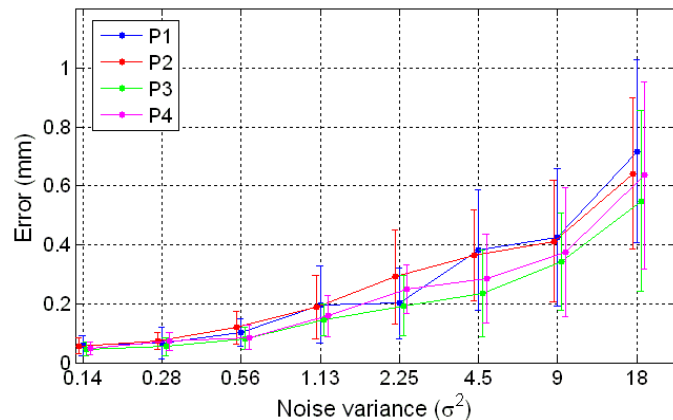
Figure 5: Error results for DLT least squares method using 20 control point pairs.

Statistically, the ANOVA test revealed main effects for *all* factors: noise variance level ($p < 0.001$), point location ($p = 0.038$), and method ($p < 0.001$). The effect of noise variance is expected as this factor was deliberately increased. There was also an interaction found between method and noise variance level ($p < 0.001$).

Although the effect of point location was found to be significant, post-hoc tests were inconsistent; the Dunnett's T3 test showed that no point location had an error significantly different than the others. Post-hoc tests also revealed that there is in fact no significant difference between the analytical method and the DLT LS method using 4 control point pairs ($p = 0.991$). The DLT LS method using 20 control point pairs, however, is significantly better than both of the previous two methods ($p < 0.001$ in both cases).

Using Matlab's Symbolic Toolbox, computational speed for the analytical method, was considerably longer than that of the DLT method. Computation of calibration matrices used in the analytical method was approximately 7.5 minutes per matrix computation. For the DLT LS method, computation of calibration matrices was about 0.002 seconds per matrix computation, regardless of how many control point pairs were used.

DISCUSSION & CONCLUSIONS

The following can be observed in Figs. 3, 4 and 5. Average radial error increases with increasing noise. A point's location within the image appears to have no substantial effect on the amount of error associated with its transformation into Cartesian space; at least not for the amounts of noise studied for this analysis. Differences in point spacing due to the distortion could explain the main effect found by the ANOVA test, but overall, looking at Figs. 3, 4, and 5 the effect does not seem to be a huge factor. Finally, Figs. 3 and 4 show comparable errors for all 4 transformed test points when the analytical method and the DLT LS method using 4 control point pairs are used. The DLT LS method using 20 control point pairs (Fig. 5) appears to be better than both of these two, which is supported by the statistical results.

As noise levels increase, the improvement of the DLT LS method with 20 points over the other two methods becomes greater, hence the interaction found between noise variance level and method in the post-hoc tests. The fact that the DLT LS method using 20 points produces much more accurate point mappings indicates that the use of more control point pairs for finding *T* is beneficial.

Within the noise levels expected for the proposed laser light-sectioning system ($\sigma^2 \leq 2.25$), the DLT LS method using 20 or more control point pairs would be the most optimal. The average error using this method for this noise range, as indicated in Fig. 5, is less than 0.2 mm for all 4 tested points. This is within a reasonable tolerance for the desired accuracy of the system at the current stage of development.

The processing time of the DLT method was considerably shorter than the analytical method. Clearly, the solution to the over-determined system of matrix equations in (4) converges very quickly. It should be noted that the calibration matrix is only computed *once* for a given camera setup, and used thereafter for transforming all data points lying along the laser traces captured by the camera. For this system, the difference in computation time between these two methods is therefore not necessarily an important factor when comparing the two approaches.

The current prototype has already demonstrated sub-mm accuracy [5] and additional work is being done to refine the accuracy for testing and validation in biomedical applications.

REFERENCES

[1] M.Y. Hajeer, D.T. Millett, A.F. Ayoub, and J.P. Siebert, "Applications of 3D imaging in orthodontics: Part I," *J. of Orthodontics*, vol.31, pp.62–70, 2004.

[2] R.J. Hennessy, S. McLearie, and A. Kinsella, "Facial surface analysis by 3D laser scanning and geometric morphometrics in relation to sexual dimorphism in cerebral–craniofacial morphogenesis and cognitive function," *J. of Anatomy*, vol.207, pp.283–295, 2005.

[3] N.H. Trinh, J. Lester, B.C. Fleming, G. Tung, and B.B. Kimia, "Accurate measurement of cartilage morphology using a 3D laser scanner," in *Proc. of 2nd Int'l ECCV Workshop on Computer Vision Approaches to Medical Image Analysis (CVAMIA '06)*, Graz, Austria, pp.37-48, May 2006.

[4] Z.B. Azouz, C. Shu, R. Lepage, and M. Rioux, "Extracting main modes of human body shape variation from 3D anthropometric data", *Proc. 5th Int'l Conf. 3-D Digital Imaging and Modeling (3DIM '05),* Ottawa, Ont., Canada, pp. 335-342, June 2005.

[5] B.D. Bradley, M.J.D. Hayes, A.D.C. Chan, "A simple, low cost, 3D scanning system using the laser light-sectioning method", *accepted to IEEE Int'l Inst. Meas. Tech. Conf. (I^{2}MTC),* 2008.